

# SEMI-AUTOMATIC REGISTRATION OF 3D-MULTI-MODALITY BRAIN IMAGES BASED ON AN INFORMATION THEORETIC APPROACH

*Peter Hastreiter, Walter Hopfer, Thomas Ertl*

Universität Erlangen, Institut für Graphische Datenverarbeitung  
Am Weichselgarten 9, 91058 Erlangen, Germany  
hastreiter@informatik.uni-erlangen.de

## ABSTRACT

For the retrospective, rigid body registration of two 3D datasets from different modalities (MR, CT and PET) an automatic, voxel based approach, as suggested by Collignon et al. [3], was implemented using mutual information of grey-value pairs as a measure of similarity. The applied information theoretic approach combines the segmentation of features and the consecutive registration in one process. By introducing a resolution pyramid and a threshold we accelerated the registration process and made it more robust with respect to the partial volume effect. In order to obtain good starting values we used a least square point matching approach based on approximately corresponding anatomical landmarks. Our results show that good registration can be achieved for MRI-MRA, MRI-CT and MRI-PET even in case of big partial volume effect.

## 1. INTRODUCTION

In many clinical situations in neuroradiology the fusion of images from different modalities taken at different times represents an important prerequisite for optimal diagnosis and therapy planning. Depending on the clinical requirements, it is not sufficient to consider anatomy, morphology or functional information derived from MR, CT or PET in separate datasets but to fuse and visualize the information in one dataset. Due to different resolution, position and orientation of 3D datasets a transformation of the coordinate system of the floating dataset to the coordinate system of the reference dataset is required in a first step. Therefore, a retrospective, rigid-body, voxel-based approach was implemented which allows for the registration of two 3D datasets. In comparison to other registration methods this approach is supposed to work for various medical imaging modalities like MR, CT or PET and should in general not be restricted to specific modalities.

Reviews of different approaches for solving the registration problem are presented by Maurer [7], van

den Elsen [10] and Brown [1] who primarily distinguish between two main concepts. The first group of algorithms is clustered around artificial, extrinsic image properties employing various kinds of frames, masks or skin markers and must therefore be classified as non-retrospective. On the contrary, there are many very popular approaches using all kinds of intrinsic image properties. This second group may further be subdivided into methods based on point landmarks, corresponding structures, moments and principle axis or on voxel-similarity.

Still, the highest matching-precision and fastest registration results can be guaranteed by using approaches on extrinsic markers because segmentation of corresponding landmarks is not as difficult as with anatomical information. However, there is a great demand for approaches using intrinsic information exclusively due to their retrospective character and much better patient friendliness.

Point- and surface-based algorithms seem to be most popular among retrospective approaches which is certainly justified for data representing anatomical information like MR and CT. However, in this case a separate segmentation step is necessary in order to receive corresponding structures on which the actual matching can be performed. In the contrary to that, if functional information like PET is involved, it seems to be much more appropriate to use voxel-based concepts [3, 5, 11] which make use of all the inherent voxel-information of the involved datasets exhibiting a much more global character. For other modalities like MR-CT a voxel-based approach also seems to be useful because the process of segmentation is already incorporated within the registration.

In general with voxel-based methods, the grey-values of all voxels are taken into account in order to optimize a function which measures the similarity of voxel pairs. A preliminary segmentation step which actually represents the basis for point- and surface-based methods and which is a main source for registration errors can be omitted because it is now part of the registration process. However, simple correla-

tion of grey-values only works correctly if there is a linear mapping between the involved datasets. Most of the voxel-based approaches [5, 11] presented so far are heuristic in nature assuming that the mapping of the grey-values is an explicit functional description.

Recently, a very promising information theoretic approach was presented by Collignon et al. [2, 3] which takes the mutual information of the joint probability distribution of the grey values of two 3D datasets as a measure for the registration solution. This approach is supposed to be more robust than any of the surface-based or heuristic voxel-based approaches and should also be more stable with respect to the problem of partial overlap.

In the first part of this paper we will present some of the important aspects of information theory. In a second part we discuss the method and the registration algorithm as well as some details of our implementation. Finally, we will present our results working with MRI-MRA, MRI-CT and MRI-PET datasets and discuss some of the experiences made.

## 2. THEORY AND METHOD

Medical tomography datasets of the head like MR, CT or PET represent the anatomical, morphological or functional situation. Neglecting the 3D nature of the datasets and reading out the voxels in a pre-defined sequence, a discrete signal is obtained with the grey-values representing the signal amplitude and the position within this sequence being analogous to a time interval. According to this interpretation the problem of registration can be mapped to the *source-channel-drain* model of information theory including all the theoretical framework which is available. Applied to the model one dataset is chosen as information source and the other as information drain while the registration transformation represents the channel.

Some basic quantities which can be derived from the signal at the source of the channel are the *information content*  $I$  of a message and its *mean information content*  $H$ .

According to Shannon the information source  $X$  represented by  $m$  different signals  $\{x_1, x_2, \dots, x_m\}$  each of which occurring with a certain probability  $p(x)$  is defined by

$$I(x) = \log_2\left(\frac{1}{p(x)}\right). \quad (1)$$

An approximation of the actual entropy is the mean information content of the information source. It is defined as

$$H(X) = \sum_{x \in X} p(x) \log_2\left(\frac{1}{p(x)}\right). \quad (2)$$

Similarly, the drain  $Y$  of the information channel is represented by  $n$  different signals  $\{y_1, y_2, \dots, y_n\}$  and may be assigned the information content according to

$$I(y) = \log_2\left(\frac{1}{p(y)}\right). \quad (3)$$

In the same way as with the information source the mean information content of the drain is defined as

$$H(Y) = \sum_{y \in Y} p(y) \log_2\left(\frac{1}{p(y)}\right). \quad (4)$$

Concerning the registration problem,  $X$  represents the dataset at the source and  $Y$  the dataset at the drain. Since the two datasets are of different modality,  $X$  and  $Y$  are stochastically independent including the fact that they are only linked by the registration transformation which substitutes the information channel. This is the reason why there should be a value which measures the amount of transferred information if there was a signal  $x$  at the source and a signal  $y$  at the drain. As a result of these considerations the expression

$$\begin{aligned} I(X, Y) &= \log_2\left(\frac{1}{p(x)}\right) - \log_2\left(\frac{1}{p(x|y)}\right) \\ &= \log_2\left(\frac{1}{p(x)}\right) - \log_2\left(\frac{p(y)}{p(x, y)}\right) \\ &= \log_2\left(\frac{p(x, y)}{p(x)p(y)}\right) \end{aligned} \quad (5)$$

is obtained where the *Law of Bayes* is applied relating the joint probability  $p(x, y)$  to the conditional probability  $p(x|y)$ .

Consequently, the *mutual information* or *Shannon information*  $S(X, Y)$  is defined by summing for all pairs  $(x, y)$

$$S(X, Y) = \sum_{(x, y)} p(x, y) \log_2\left(\frac{p(x, y)}{p(x)p(y)}\right) \quad (6)$$

with the marginal probabilities  $p(x)$ ,  $p(y)$  and the joint probability  $p(x, y)$ .

The basis for all these assumptions is the fact that the 2D histogram of two exactly aligned datasets will be dispersed if one of the datasets is moved away from the registration solution [5, 11]. According to Collignon et al. [3] this degree of dispersion can be measured with mutual information because the interpretation of the included properties shows that the lower limit of equation (6) is reached with complete independence and the upper limit with complete interdependence of the two datasets to be matched.

### 3. ALGORITHM AND IMPLEMENTATION

The definition of *mutual information* according to equation (6) has to be adapted to the problem of registering two datasets of different modalities. The abstract signal  $X$  at the source is substituted by a volume dataset with the grey-levels  $f_X(s)$  and with  $s$  representing the coordinates of the voxels. The probability  $p(x)$  may then be obtained by simple summation and normalization of the grey-values. In order to calculate the joint probability  $p(x, y)$  and the probability  $p(y)$  of the drain dataset with grey-levels  $f_Y(s)$  the voxels of the drain dataset must be known which are covered after applying the registration transformation  $T_\alpha$  to the voxels of the source dataset with the parameters of  $T$  changing according to the value of mutual information  $\alpha$  for every iteration. The values for  $p(y)$  and  $p(x, y)$  may then be determined respectively by simple summation and normalization of the voxels included. These considerations lead to the following equation with  $\alpha_{opt}$  representing the transformation parameters where the minimum of the mutual information is found by an optimization algorithm:

$$\alpha_{opt} = \min_{\alpha} \left( - \sum_s p(f_X(T_\alpha s), f_Y(s)) \cdot \log_2 \left[ \frac{p(f_X(T_\alpha s), f_Y(s))}{p(f_X(T_\alpha s))p(f_Y(s))} \right] \right) \quad (7)$$

Since we are using this registration scheme for head data exclusively we restricted the transformation  $T$  to three translations and three rotations by applying the rigid body assumption which is regarded to be well satisfied according [3].

Transforming a voxel of the source dataset does usually not lead to an exact voxel position in the drain dataset. The fastest solution for this interpolation problem could be nearest neighbor interpolation. However, as a disadvantage the parameters of the calculated transformation will then not change continuously. Alternatively, a trilinear interpolation could be used instead. This is, however, not suitable either because the calculation of grey-levels at inter-voxel positions leads to an artificial dispersion of the grey-level histogram. This would falsify the result of equation (7) after numerical optimization.

Collignon et al. [3] therefore proposed an interpolation procedure called *partial-volume-distribution* which also requires the weights derived from trilinear interpolation. Contrarily, the weights are now used to update the joint 2D-histogram of the datasets and in the same way to update the probabilities  $p(x)$ ,  $p(y)$ ,  $p(x, y)$ . If a voxel of the drain dataset is inside the transformed volume of the source dataset its corresponding weights are added to the entry of the joint histogram, to the entry of the source dataset histogram and finally to the entry of the drain dataset histogram.

In our implementation the optimization of the mutual information according to equation (7) is performed by Powell's algorithm [8] and will therefore just find a local minimum. Since we are applying a preprocessing step in order to find initial values for the transformation parameters in the vicinity of the registration solution the result of the optimization can be interpreted as optimal if the local minimum  $\alpha_{opt}$  is reached.

Due to the problem of local minima occurring with the calculation of mutual information we simply used the technique of corresponding landmarks in order to find starting values for the parameters of the optimization algorithm. This method proved to be satisfactory even in case of complementary information like with MR-CT or MR-PET. Since this method is not required to provide a good registration a quick selection of approximately corresponding landmarks was sufficient.

By introducing a resolution pyramid consisting of three levels we could accelerate the process of optimization during the first step. We simply used every fourth voxel along each axis for the first level and every second voxel for the second level before calculating with full resolution in the final level. Reducing the amount of voxels in the beginning was very useful in order to quickly approach the optimal value of mutual information.

### 4. RESULTS AND DISCUSSION

In order to test our implementation we used the following datasets:

1. For a test of functionality a (256 x 256 x 128) MRI dataset (voxel size: 0.99 x 0.99 x 1.36 mm) at the source and a copy of it which was displaced by (7.0, 6.0, 10.0) mm and rotated by (10.0, 5.0, 5.0) degrees was used. As a result, the optimization algorithm returned the registration parameters with an error of less than 1%.
2. For a second test the same MRI dataset was applied together with a corresponding (256 x 256 x 72) MRA dataset (voxel size: 0.89 x 0.89 x 0.94 mm). The result of the registration can be seen in Fig. 2, 3 and 4. The darker areas show the MRA parts.
3. Testing the algorithm with complementary information we used a (256 x 256 x 30) MRI dataset (voxel size: 1.33 x 1.33 x 4.0 mm) together with a corresponding (256 x 256 x 40) CT dataset (voxel size: 1.33 x 1.33 x 4.0 mm). The result of this test can be seen in Fig. 6, 7 and 8.

4. For a final test with complementary information we used a (256 x 256 x 55) MR dataset (voxel size: 0.86 x 0.86 x 2.5 mm) and a corresponding (128 x 128 x 31) PET dataset (voxel size: 2.0 x 2.0 x 3.38 mm) with the result of the matching visualized in Fig. 10, 11 and 12.

Initially, the algorithm was very sensitive to the problem of partial overlap even if the volumes to match were close to the registration solution. This problem could only be overcome by introducing a threshold in order to suppress the influence of background noise which restricted the overlapping part of the volumes to the essential information.

In order to examine the behaviour of the algorithm in the vicinity of the registration solution one of the datasets was rotated around the main axes ( $X, Y, Z$ ) after registration. The respective values of mutual information were plotted in Fig. 1, 5 and 9. Especially for our MRI - PET data some significant local minima occurred at 90 and 180 degrees which are, to our opinion, due to symmetry effects. For our MRI - CT data an additional minimum could only be found at 180 degrees because the missing upper part of the head in the MR dataset reduced the influence of symmetry at 90 degrees. Since the MRA dataset of our MRI - MRA data only covers the center part of the head a possible minimum at 180 degrees is almost negligible. Due to these minima it was essential to find starting values close to the registration solution. We achieved this by a quick selection of approximately corresponding landmarks which proved to be sufficient because only the shape based symmetry effects had to be overcome.

The additional introduction of a simple resolution pyramid in order to approach the vicinity of the registration solution accelerated our implementation by a factor of two. The whole matching took 1h 15 min (level one: 2 min, level two: 15 min) for our MRI-MRA data and 25 min (level one: 1 min, level two: 5 min) for our MRI-CT data running on a 250 MHz SGI Indigo<sup>2</sup>.

Up to this stage the precision of our algorithm may only be checked visually. This, however, is not a real drawback since visual inspection of the results is an important technique for evaluation. According to Hemler et al. [4] several problems remain concerning the determination of the accuracy of registered data. As proposed, the solution to this problem could be a reference dataset with internally placed markers.

## 5. CONCLUSION

Mutual information as presented by Collignon et al. [3] was successfully applied to a diversity of modalities like MRI-MRA, MRI-CT and MRI-PET. Taking

into account the visually inspected results of our implementation it turns out to be a data independent measure and produces fairly good results without an initial segmentation step which is usually sensitive to segmentation errors. However, finding appropriate initial parameters was essential due to symmetry effects which cause local minima in the vicinity of the registration solution. Introducing a threshold and a simple resolution pyramid was necessary to make the algorithm less sensitive to the problem of partial volume effect and to accelerate the performance of the algorithm by a factor of two. Still, further tests have to be performed including comparisons with other matching procedures and data with a stereotactic frame. As a final task the procedure for finding the starting values should be automated and the approach be extended to fully affine transformations.

## 6. REFERENCES

- [1] L.G. Brown, *A survey of image registration techniques*, ACM Computing Surveys, Vol. 24, No. 4, pp. 325-376, Dez. 1992
- [2] A. Collignon, D. Vandermeulen, P. Suetens, G. Marchal, *3D Multi-Modality Medical Image Registration Using Feature Space Clustering*, in: Lecture Notes in Computer Science 905, Springer, pp. 195-204, 1995.
- [3] A. Collignon, F. Maes, D. Delaere, D. Vandermeulen, P. Suetens, G. Marchal *Automated multi-modality image registration based on information theory*, in: Kluwer Acad. Publ's: Computational Imaging and Vision, Vol.3, pp. 263-274, 1995
- [4] P.F. Hemler, S. Napel, T.S. Sumanaweera, R. Pichumani, P.A. van den Elsen, D. Martin, J. Drace, J.R. Adler, *Registration error quantification of a surface based multimodality images fusion system*, Med. Phys. 22(7), pp. 1049-1056, July 1995.
- [5] D.L.G. Hill, *Combination of 3D medical images from multiple modalities*, Ph.D. Thesis, University of London, Dec. 1993.
- [6] D.L.G. Hill, C. Studholm, D.J. Hawkes, *Voxel Similarity Measure for Automated Image Registration*, Proc. SPIE Vol. 2359, Visualization in Biomedical Computing, SPIE Press, Bellingham, WA, Rochester, Oct. 1994.
- [7] C.R. Maurer, J.M. Fitzpatrick, *A Review of medical image registration*, Interactive Image-Guided Surgery, Maciunas, R.J. (Ed), Park Ridge, IL, American Association of Neurological Surgeons, pp. 17-44, 1993.
- [8] W.H. Press, B.P. Flannery, S.A. Teukolsky,

W.T. Vetterling, *Numerical Recipes in C*, The Art of Scientific Computing, Cambridge University Press, 1988.

- [9] P.A. van den Elsen, *Multimodality Matching of Brain Images*, Ph.D. Thesis, Utrecht University Thesis, June 1993.
- [10] P.A. van den Elsen, E.-J.D. Pol, M.A. Viergever, *Medical Image Matching - A Review with Classification*, IEEE Eng. in Medicine and Biol., pp. 26-38, March 1993.
- [11] R.P. Woods, J.C. Mazziotta, S.R. Cherry, *MRI-PET Registration with Automated Algorithm*, JCAT, 17(4):536-546, July/August, 1993.
- [12] M. Bossert, *Kanalcodierung*, Teubner Verlag, Stuttgart, 1992.

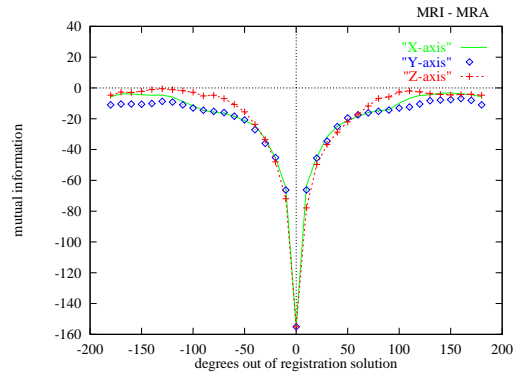


Figure 1: Value of mutual information if one dataset is twisted out of the registration solution around main axis X, Y, Z.

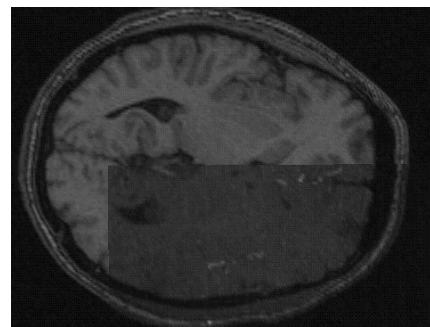


Figure 2: axial slice

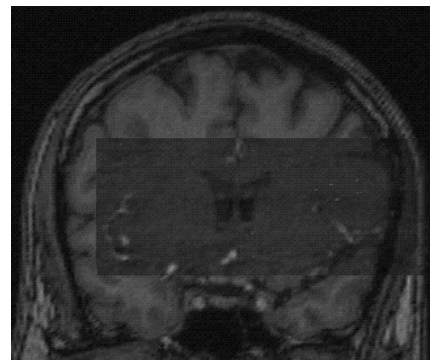


Figure 3: coronal slice



Figure 4: sagittal slice

Registration results with MRI-MRA

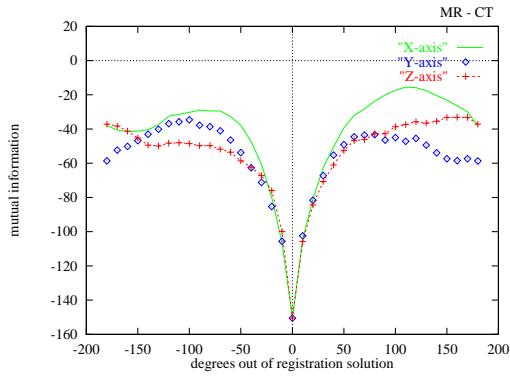


Figure 5: Value of mutual information if one dataset is twisted out of the registration solution around main axis X, Y, Z.

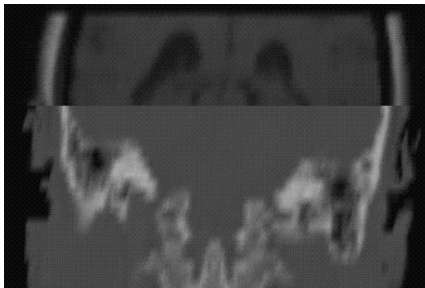


Figure 6: coronal slice

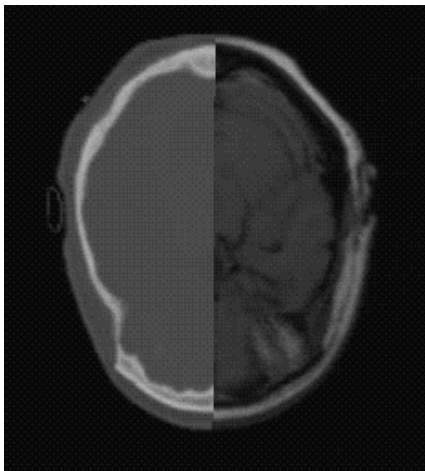


Figure 7: axial slice

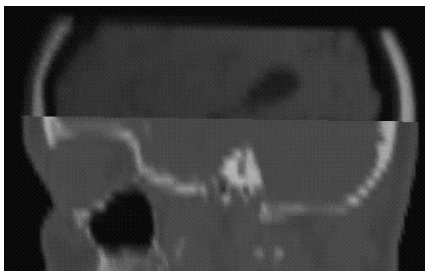


Figure 8: sagittal slice

Registration results with MRI-CT

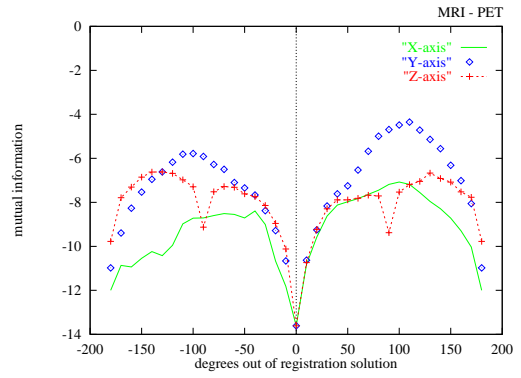


Figure 9: Value of mutual information if one dataset is twisted out of the registration solution around main axis X, Y, Z.

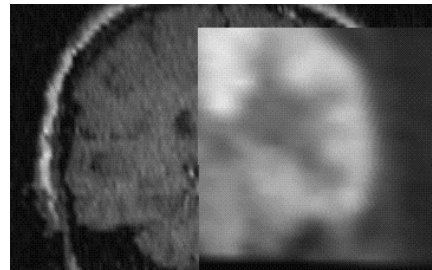


Figure 10: coronal slice

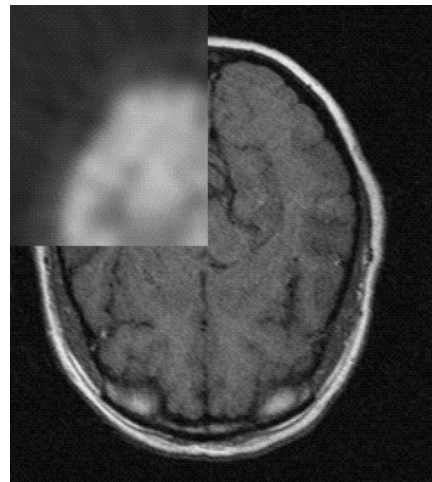


Figure 11: axial slice

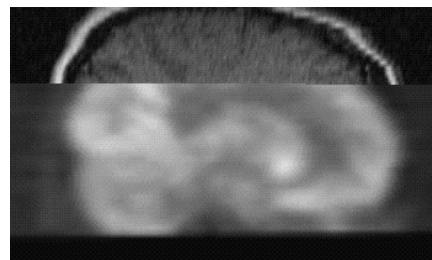


Figure 12: sagittal slice

Registration results with MRI-PET